



Pyruvate carboxylase deficiency type A and type C: Characterization of five novel pathogenic variants in *PC* and analysis of the genotype–phenotype correlation

Emanuele G. Coci^{1,2}  | Vytautas Gapsys³ | Natasha Shur^{4,5} | Yoon Shin-Podskarbi⁶ | Bert L. de Groot³ | Kathryn Miller⁴ | Jerry Vockley⁷ | Neal Sondheimer⁸ | Rebecca Ganetzky⁹  | Peter Freisinger¹⁰

¹Department for Neuropediatrics, University Children's Hospital, Ruhr University Bochum, Bochum, Germany

²Institute for Neuropediatrics and Social Pediatrics, Hamburg, Germany

³Computational Biomolecular Dynamics Group, Max Plank Institute for Biophysical Chemistry, Göttingen, Germany

⁴Division of Genetics, Albany Medical Center, Albany, New York

⁵Children's National Medical Center, Washington, District of Columbia

⁶Molecular Genetics and Metabolism Laboratory, Munich, Germany

⁷Children's Hospital of Pittsburgh, University of Pittsburgh School of Medicine, Pittsburgh, Pennsylvania

⁸Clinical and Metabolic Genetics, The Hospital for Sick Children, Toronto, Ontario, Canada

⁹Division of Human Genetics, Children's Hospital of Philadelphia, Philadelphia, Pennsylvania

¹⁰Department of Pediatrics, Klinikum Reutlingen, Reutlingen, Germany

Correspondence

Emanuele G. Coci, Institute for Neuropediatrics and Social Pediatrics, Hamburg, Germany.
Email: emanuele.coci@institut-sozialpaediatric.de

Abstract

Pyruvate carboxylase deficiency (PCD) is caused by biallelic mutations of the *PC* gene. The reported clinical spectrum includes a neonatal form with early death (type B), an infantile fatal form (type A), and a late-onset form with isolated mild intellectual delay (type C). Apart from homozygous stop-codon mutations leading to type B PCD, a genotype–phenotype correlation has not otherwise been discernible. Indeed, patients harboring biallelic heterozygous variants leading to *PC* activity near zero can present either with a fatal infantile type A or with a benign late onset type C form.

In this study, we analyzed six novel patients with type A (three) and type C (three) PCD, and compared them with previously reported cases. First, we observed that type C PCD is not associated to homozygous variants in *PC*. In silico modeling was used to map former and novel variants associated to type A and C PCD, and to predict their potential effects on the enzyme structure and function. We found that variants lead to type A or type C phenotype based on the destabilization between the two major enzyme conformers. In general, our study on novel and previously reported patients improves the overall understanding on type A and C PCD.

KEYWORDS

biotin carboxyl carrier protein domain, biotin carboxylase domain, carboxyl transferase domain, neurodevelopmental delay, *PC* tetramerization domain, pyruvate carboxylase, pyruvate carboxylase deficiency

1 | INTRODUCTION

Pyruvate carboxylase deficiency (PCD; MIM# 266150) is a rare recessive genetic disorder (estimated prevalence 1:250,000) affecting the confluence of glucose metabolism, lipogenesis, and neurotransmitter synthesis (Wang et al., 2009). The pyruvate carboxylase (*PC*) gene maps to 11q13.2 and consists of four noncoding exons and

20 coding exons. No pseudogenes are known. Three tissue-specific variant transcripts differ from each other at the 5'-untranslated region region but encode the same 1,178 amino acid protein (in addition to the 20 amino acid mitochondrial leader sequence) containing three domains (biotin carboxylation, [BC]; transcarboxylation, [CT]; and biotin carboxyl carrier, [BCCP]) and two spacer regions (Wallace, Jitrapakdee, & Chapman-Smith, 1998). *PC* is a

homotetramer localized to the mitochondrial matrix and converts pyruvate into oxaloacetate. PC structures resolved by means of X-ray crystallography suggest that the protein undergoes large conformational transitions over the course of its two-step enzymatic reaction (St Maurice et al., 2007; Xiang & Tong, 2008). In the first step, a biotin moiety covalently bound to the BCCP domain is carboxylated. This step requires adenosine triphosphate (ATP), whereas binds to the BC domain and is allosterically activated by acetyl-CoA. In the second step, biotin transfers a carboxyl group to pyruvate. This reaction takes place at the CT domain. The active sites of the BC and CT domains are separated by more than 70 Å in the PC structures of *Staphylococcus aureus* and *Rhizobium etli*. Biotin translocation requires large scale molecular motion of the BCCP domain between the BC and CT domains.

Mitochondrial oxaloacetate participates in several critical biochemical pathways. It is converted into aspartate, required for protein synthesis, for the production of argininosuccinate, a metabolite of urea cycle, and for the conversion of glutamate into the neurotransmitter γ -aminobutyric acid (GABA). Oxaloacetate is a component of the tricarboxylic acid (TCA; Krebs's) cycle, and its absence leads to a reduction of mitochondrial nicotinamide adenine dinucleotide, a substrate of complex I of the respiratory chain. During fasting, oxaloacetate is converted into phosphoenolpyruvate, required for gluconeogenesis. Finally, oxaloacetate is necessary for the transport of mitochondrial acetyl-CoA into the cytoplasm, where it participates in the synthesis of fatty acids. Taken together, lack of oxaloacetate due to PCD has a plethora of severe metabolic consequences (Marin-Valencia, Roe, & Pascual, 2010).

Two clinical subtypes with early onset and fatal outcomes have been defined: A (also called "American type") and B (also called "French type"). Type A PCD manifests several months after birth and presents with increasing generalized developmental delay and hypotonia, failure to thrive, profound apathy, and intermittent lactic acidemia with intercurrent illnesses or other physiologic stress (e.g., infections). All reported patients have died during infancy or early childhood. Few patients with this infantile and always fatal PCD form were reported in the literature (Ahmad et al., 1999; Monnot et al., 2009; Robinson et al., 1987; Wang et al., 2008).

Type B PCD presents in the first hours after birth with severe lactic acidosis, hyperammonia, hypercitrullinemia, and hypoglycemia. Immediately following birth, neurological status and consciousness level are typically normal, but after 1–72 hr a hypokinetic-rigid syndrome with profound axial hypotonia appears, which is accompanied by a tremor of the limbs and bizarre ocular movements in some patients. During the first months of life, increasing liver insufficiency and seizures develop in some patients. Patients die within 5 months after birth (Carbone, Applegarth, & Robinson, 2002; Carbone et al., 1998). Only 38 inactivating mutations in the PC gene have been described in patients with type A and B PCD (Breen et al., 2014; Carbone et al., 1998, 2002; Monnot et al., 2009; Ortez et al., 2013; Wang et al., 2008; Wexler et al., 1998). Several other PCD patients have been reported based on biochemical stigmata of PCD and/or on reduction of pyruvate carboxylase activity, but without

molecular confirmation of the diagnosis (Ahmad et al., 1999; Arnold, Griebel, Porterfield, & Brewster, 2001; Brun et al., 1999; Hamilton, Rae, Logan, & Robinson, 1997; Oizumi et al., 1983; Pineda et al., 1995; Robinson et al., 1987; Van Coster, Fernhoff, & De Vivo, 1991; Van Coster, Janssens, Misson, Verloes, & Leroy, 1998).

Therapeutic options for type A and B disease are limited. Anaplerotic diet or compounds (e.g., triheptanoin, citrate, or aspartate) have shown variable success in reducing metabolic derangements, but have not achieved an amelioration of the neurological symptoms and a prolongation of life span (Breen et al., 2014; García-Cazorla et al., 2006; Mochel et al., 2005).

The third form of PCD (type C or benign) is characterized by short episodes of ketoacidosis during infancy and childhood, typically associated with intercurrent illnesses, mild psychological delay and neurologic symptoms, and survival until late adolescence in the six reported patients (Arnold et al., 2001; Hamilton et al., 1997; Higgins, Glasgow, Lusk, & Kerr, 1994; Higgins, Ide, Oghalai, & Polymeropoulos, 1997; Schiff et al., 2006; Van Coster et al., 1991; Wang et al., 2008). PCD mutations were reported in only two cases (Wang et al., 2008). Enzymatic activity was reported as 1–10% (of healthy control) in skin fibroblasts or peripheral blood leukocytes in three patients (Arnold et al., 2001; Hamilton et al., 1997; Van Coster et al., 1991), below 1% in two patients (Schiff et al., 2006; Wang et al., 2008) and was unreported in one patient (Wang et al., 2008). Thus, the residual enzymatic activity does not appear to be a reliable prognostic parameter in this condition.

Reported genotype/phenotype correlations in both fatal PCD forms (infantile type A and neonatal type B) have been inconsistent. Initially, it appeared that the presence of at least one truncating mutation in the PC gene led to type B presentation, while biallelic missense mutations lead to type A (Carbone et al., 1998, 2002; Monnot et al., 2009). However, additional reports have not been as clear, with type B presentation seen in patients with biallelic missense mutations (Breen et al., 2014; Ostergard et al., 2012; Wang et al., 2008). Moreover, Wang et al. (2008) hypothesized that mosaicism for mutations in CNS tissues correlated with patient survival.

The genetic difference between type A and C PCD has not been elucidated. Although biallelic mutations in PC have been reported in both, there has not been a clear correlation of genotype with phenotype. The prognosis among type A and type C patients is generally different, dying the former within the first years of life and surviving the latter sometimes until adulthood.

In the current study, we analyzed clinical, electrophysiological, neuroradiological, biochemical, and genetic findings in six patients with PCD, three with type A (patients 1, 2, and 3) and three with type C (patients 4, 5, and 6) PCD. The patients harbor five novel and one known pathogenic variant in PC. We compared the genetic features of these six novel patients with the previously reported type A and type C patients. We created homology models for the full structure of human PC representing two main conformations of the enzyme, where either the BCCP domain is in the vicinity of BC domain or the BCCP domain is adjacent to the CT domain, and we mapped most of

the reported mutations associated with type A and type C PCD onto the models. Together with interpolation of motion between the two structural states of the enzyme, the mapped mutations provided structural insights into the potential effects on the enzyme's function.

Taken together, this study aims to shed further light into the still unclear genotype-phenotype correlation for type A and type C PCD and to provide future PCD patients with a clearer prognosis basing on the revealed genetic mutations.

2 | PATIENTS AND METHODS

2.1 | Patients

Six patients were recruited worldwide from treating metabolic medicine physicians and were included in the study according to clinical and biochemical signs of type A or type C PCD.

2.2 | Magnetic resonance imaging (MRI) scan

For patients 1, 3, and 4, brain MRI was performed on a 3-T MR scanner using a standard clinical protocol. For patient 2, brain imaging with spectrography was performed on a 1.5-T MR scanner using a standard clinical protocol.

2.3 | Gene sequencing

Sanger sequencing of *PC*'s coding sequence and boundary regions was performed on peripheral blood leucocytes DNA by commercial testing labs using standard protocols. Genbank accession numbers are NM_001040716.1, NG_008319.1 and NP_001035806.1. The variant URLs are <https://www.ncbi.nlm.nih.gov/clinvar/variation/2094/>, https://mseqdr.org/variant.php?MSCV_0005596, https://mseqdr.org/variant.php?MSCV_0005613, <https://databases.lovd.nl/shared/variants/0000446154>, <https://databases.lovd.nl/shared/variants/0000453984>, <https://databases.lovd.nl/shared/variants/0000446155>.

2.4 | PC enzymatic activity

In patients 2, 3, and 4, the enzymatic activity of pyruvate carboxylase activity was measured in cultured skin fibroblasts from patients 2, 3, and 4 according to standard protocols (Atkin, Utter, & Weinberg 1979; Robinson et al., 1985). In patients 1, 5, and 6, the enzymatic activity in skin fibroblasts could not be measured due to either technical issues or lack of parental consent.

2.5 | Pyruvate carboxylase modeling and variant mapping

Two major conformers of the PC enzyme were modeled to mimic the functional states of biotin carboxylation (conformer 1, PDB ID 2qfc; St Maurice et al., 2007) and carboxyl transfer to pyruvate (conformer 2, PDB ID 3bg3 and 3bg5; Xiang & Tong, 2008). In the conformer 1,

BCCP domain is adjacent to the BC domain; in the conformer 2, BCCP domain is adjacent to the CT domain. All the homology modeling was performed using Modeller 9.15 (Sali & Blundell, 1993). The previously reported mutations as well as the novel mutations associated with type A and type C PCD were mapped onto the modeled structures. The structures were visualized by means of Pymol Schrödinger. The PyMOL molecular graphics system, Version 1.8.0.3, LLC. The artificial motion connecting the two modeled conformers was constructed by linearly interpolating between the structures along the difference vector between them. For a detailed description of PC modeling methods, we refer to "the supplementary material and methods".

2.6 | Free energy calculations and PC stability

The changes in PC stability upon each mutation were estimated by the established Rosetta protocol (Kellogg, Leaver-Fay, & Baker, 2011) using the Cartesian version of the method (Alford et al., 2017). Two Rosetta energy functions were used for calculations (Talaris2014 and ref2015; Alford et al., 2017): the calculated values are reported as a range between the two obtained estimates. The free energy difference ($\Delta\Delta G$) was calculated upon each type A and type C variant previously reported in the literature as well as in this study. The $\Delta\Delta G$ values were separately calculated for both conformers 1 and 2, including all the possible monomer combinations for the heterozygous and homozygous variant scenarios. The difference ($\Delta\Delta\Delta G$) among $\Delta\Delta G_{\text{conformer1}}$ and $\Delta\Delta G_{\text{conformer2}}$ is used as an indicator of the PC stability and indirectly of its functional impairment. It can be assumed that evolutionary constraints have optimized the relative stability between the conformers for carrying out the enzyme's function and a distortion of this balance, be it destabilization or over-stabilization of one conformer with respect to the other, may be viewed as an indication of the functional impairment of pyruvate carboxylase. Positive $\Delta\Delta\Delta G$ values indicate a relative stabilization of the conformer 2 with respect to the conformer 1 and negative $\Delta\Delta\Delta G$ values indicate on the contrary that the conformer 1 is more stable than the conformer 2. For a detailed description of the mathematical basis of the used thermodynamic model and the Rosetta-based calculations we refer to "the supplementary material and methods".

3 | RESULTS

3.1 | Clinical, biochemical, electrophysiological, and neuroradiological features of the patients

Patient 1 (male) is the second child of consanguineous parents and brother of a 2 years old healthy boy. Delivery at 37 weeks of pregnancy was uncomplicated, and birth weight, length and head circumference were within the normal limits. No problems were noted until 5 months of age, when he was admitted to hospital due to an acute bronchopneumonia with severe tachypnea, fever, and somnolence. He had severe lactic acidosis (serum lactate 18.1 mmol/L) and

hyperglycemia (136 mg/dl). Ammonia was 53 $\mu\text{mol/l}$ (normal range, 30–60). Organic acids analysis in urine identified elevated lactate and ketones. Initially, a defect in pyruvate dehydroxygenase complex was suspected. The patient was treated with intravenous bicarbonate and he was put on a high-fat diet (50–69%). Acidosis improved but was never completely corrected, with elevated serum lactate (7.6 mmol/L) and base excess (–4.3 mmol/L). At 7 months of age, acute metabolic acidosis occurred with respiratory syncytial virus (RSV) bronchiolitis (serum lactate 9.7 mmol/L). Currently, the patient is 11 months old with the weight of 8,280 g (10th percentile), length 71 cm (third percentile), and head circumference 45 cm (third percentile). His developmental milestones correspond to 5-months of age and he is slightly dystonic. Brain MRI performed at 6 months showed an increased signal in the putamen, globus pallidus, and caudate bilaterally (Figure 1).

Patient 2 (female) is the first child of nonconsanguineous Aboriginal Canadian parents. At birth, she suffered from lactic acidosis and generalized hypotonia. Birth weight and length were within the normal range, while head circumference was 39 cm (3 cm above 97th percentile). Until the fifth year of age, she was admitted four times due to acute metabolic acidosis and dehydration during minor intercurrent illness. Metabolic studies revealed continuously elevated levels of serum lactate (5–7.5 mmol/L and maximal peak

15 mmol/L during an infection), serum pyruvate (maximal peak 0.28 mmol/L), and alanine (750–1500 $\mu\text{mol/L}$). Base excess and pH were within the normal range between illnesses and decreased during infection-associated metabolic misbalances, the lowest measured base excess was –13 and the lowest pH was 7.13. At 2 days of age, brain MRI revealed ventriculomegaly with large subependymal cysts and pronounced serum lactate peaks in spectroscopy. Currently, she is 11.5 years old, has a weight of 45.9 kg (75th percentile), length of 147.5 cm (50th percentile), and head circumference of 52.5 cm (50th percentile). Developmental progression has arrested at approximately the stage of a 2-year-old child. The patient is able to pronounce about 10 words, but is unable to build two words sentences. She can walk and run with good coordination, and does have problems with tantrums. No psychological testing has been performed and no further developmental progression is expected. The patient has been treated with oral biotin, aspartate, carnitine, thiamine, and citrate since the diagnosis.

Patient 3 (male) is the first child of nonconsanguineous parents. The birth was uncomplicated at the 39th pregnancy week. At 3 weeks of age, bilateral clonic seizures started, lasting from 30 s to 3 min and sometimes occurring in clusters of 3–4 seizures. Oral Levetiracetam and Vigabatrin partially controlled the seizures; oral

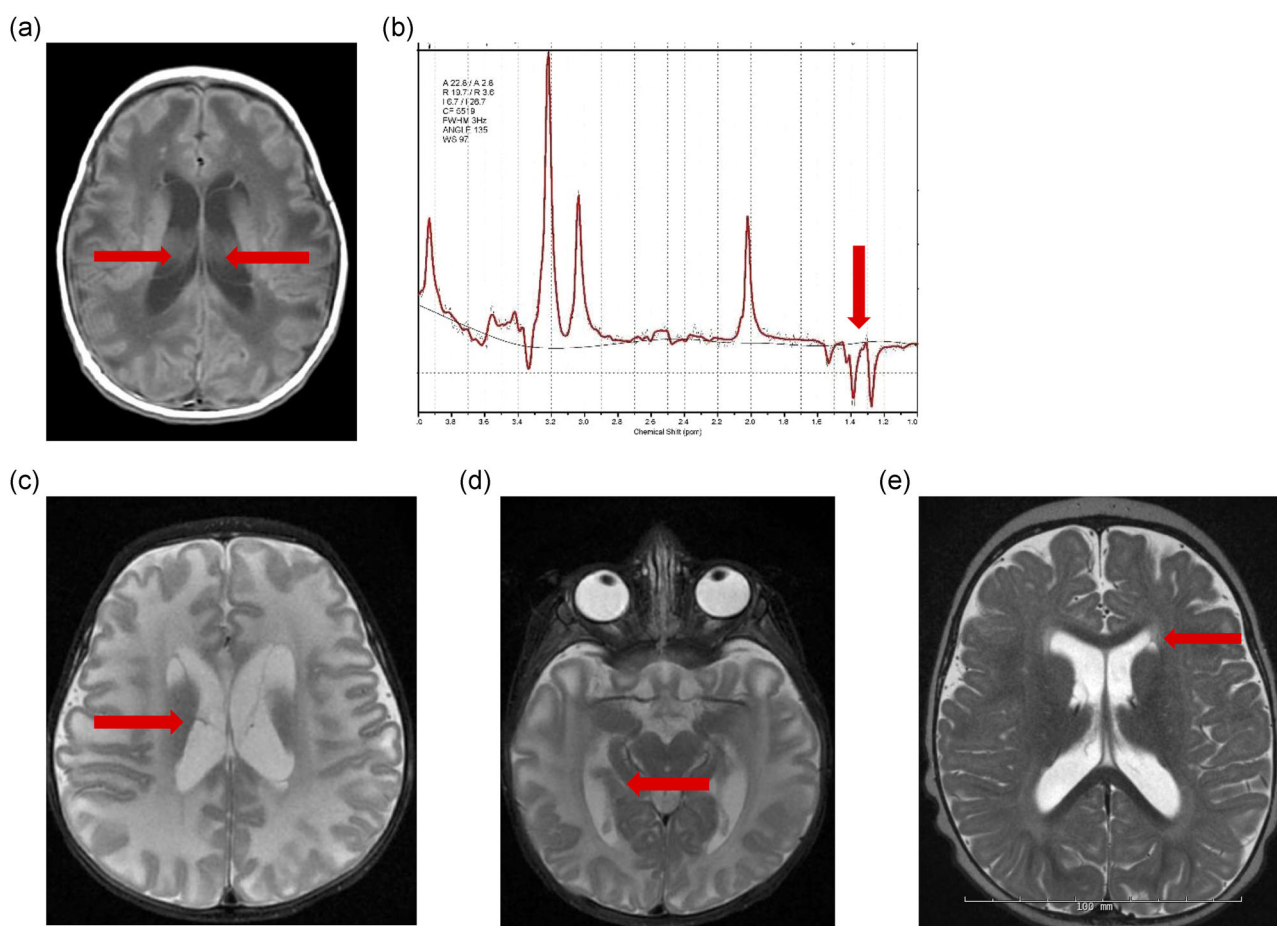


FIGURE 1 Brain MRI. Coronal cut (a) and spectrographic peaks (b) from patient 2 (type A), two coronal cuts (c and d) from patient 3 (type A), one coronal cut from patient 4 (e) (type C). The arrows indicate the structural brain abnormalities

steroids were added for 30 days due to breakthrough infantile spasms. At 6 months of age, he suffered two episodes of metabolic acidosis within a few weeks without an apparent trigger. He was somnolent and hypotonic, had increased serum lactate (10.8 mmol/L), decreased bicarbonate (11 mmol/L) and pH (7.35), normal ammonia and glucose levels and was discharged after intravenous fluid therapy. Plasma alanine, taurine, glutamic acid, glutamine, and proline were almost constantly elevated, while aspartic acid, threonine, citrulline, cystine, lysine, and histidine were intermittently elevated. In the unique cerebrospinal fluid test, alanine and citrulline were elevated. MRI investigation at 2 months of age revealed cystic change in the periventricular white matter, delayed myelination, and underpercularization of the sylvian fissures (Figure 1). At the current age of 22 months, the patient fixes objects but does not actively follow them, brings the hands to midline, takes objects with both hands and cannot sit without support. Weight and head circumference are on the 50th percentile and length is on the 75th percentile. He is currently treated with oral Biotin (10 mg daily).

Patient 4 (male) is the first child of nonconsanguineous parents. Fetal MRI revealed ventriculomegaly with septations and agenesis of the corpus callosum (Figure 1). Birth at the 40th pregnancy week and neonatal period were uncomplicated, apart from hyperbilirubinemia. At 11 months, he suffered from an acute ear infection, and then abruptly developed mental status changes, ultimately becoming comatose, and Kussmaul breathing. Having a pH 6.7 and bicarbonate 2 mmol/L, the patient was resuscitated with intravenous bicarbonate infusion. After this first metabolic crisis, he had permanently elevated levels of urinary ketone bodies and plasma pyruvate and lactate. Serial biochemical tests revealed constantly increased levels of plasma alanine and intermittently elevated levels of plasma proline and lysine. At 3, 4, and 5 years of age, the patient suffered from acute metabolic acidosis episodes in the setting of cough, RSV infection, and gastroenteritis, respectively. At the current age of 6 years, he has stereotyped movements (hand flapping), walks, jumps, climbs stairs, throws, and catches. He expresses about 10 purposeless sounds but not intelligible words, follows commands and seems to understand speech, plays, and shares with other children, distinguishes strangers from known people. Weight and length are on the 90th percentile. The patient is currently treated with biotin (10 mg daily), carnitine (50 mg/kg daily), and riboflavin (50 mg daily).

Patient 5 (male) is the second child of nonconsanguineous parents, born to nonconsanguineous parents. He was born at full-term with normal weight and length. Head circumference was at the 99th percentile. Family's clinical history was unremarkable. At 2 years of age, the child had good motor skills though he walked on his toes, but spoke only a few words. He was given a diagnosis of autism spectrum disorder because of poor eye contact and obsessive behaviour. He subsequently presented at that age to the emergency department with increased work of breathing and significant retractions with afebrile illness and upper respiratory infection. The metabolic evaluation revealed pH 7.07, bicarbonate 6 mmol/L, serum lactate 8.27 mmol/L, and ammonia 45 μ mol/L, which normalized with therapy. After paediatric intensive care with intravenous bicarbonate

and fluid therapy, pH stabilized to normal. Retrospectively, a smell of ketosis on his breath was reported. He subsequently has had two additional episodes of metabolic acidosis with increased serum lactate (13 and 16 mmol/L) corrected with intensive fluid therapy. Currently, he is 3 years old, has a weight of 15.5 kg (67th percentile), length of 99 cm (72th percentile), and head circumference of 52 cm (98th percentile). After starting oral triheptanoin (30 g daily, ~ 2 g \cdot kg $^{-1}\cdot$ d $^{-1}$) at 3 years of age, he is reported to have increased speech and improved eye contact.

Patient 6 (male) is the younger brother of patient 5. He was born full-term without complication and has not had any motor delay. Because of his brother's clinical history, he was tested at birth and found to have the same PC variants as his older brother after his diagnosis. He is currently 16 months old, and his weight is 10.8 kg (60th percentile), length 77.5 cm (17th percentile), and head circumference 47.7 cm (71st percentile). He is babbling and interacting more than his brother, however, he is not yet pointing. He has not had any episodes of metabolic decompensation even during illnesses. On routine testing, the patient 6 has increased lactic acid (6.3 mmol/L) and decreased bicarbonate (17 mmol/L). He was started oral triheptanoin at age 2 months and is currently getting 15 mg/d (1.5 g \cdot kg $^{-1}\cdot$ d $^{-1}$).

3.2 | PC variants and enzymatic activity of pyruvate carboxylase

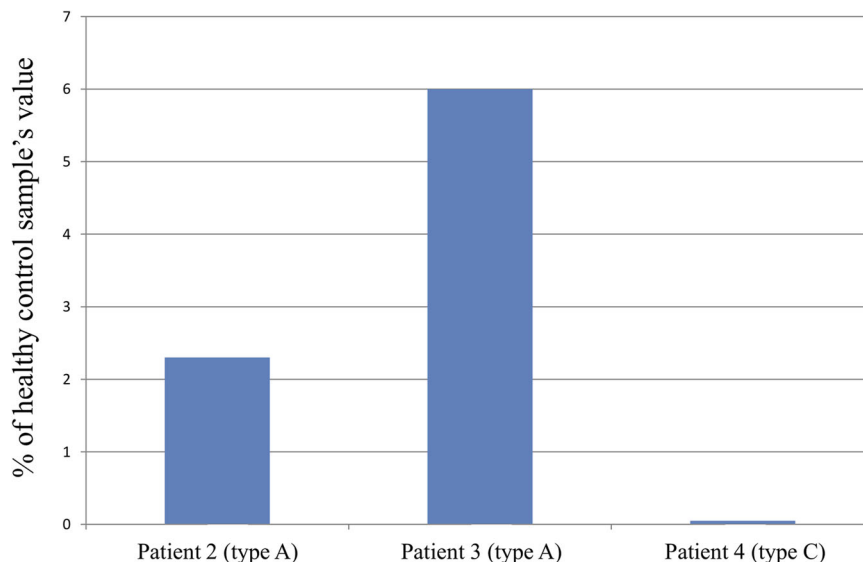
In patient 1 (type A), PC harbors the duplication of c.449_451GGA in homozygous state. Both parents are heterozygous for c.449_451GGA. The encoded protein includes an additional glycine 151 after wild-type glycine 150. Enzymatic activity of pyruvate carboxylase could not be measured due to technical issues of testing.

Genetic testing of patient 2 (type A) revealed the homozygous variant c.1828G>A in PC, which causes the exchange of alanine 610 into threonine. Both parents are heterozygous for this variant. This mutation was already described in Indo-Americans from Canadian Cree and Ojibway tribes and was only associated to type A PCD. Enzymatic activity of pyruvate carboxylase measured in skin fibroblasts was 0.02 nm \cdot min $^{-1}\cdot$ mg $^{-1}$ protein (2.3% of control sample; control = 0.87 \pm 0.32 nm \cdot min $^{-1}\cdot$ mg $^{-1}$; Figure 2).

Patient 3 (type A) harbors c.1877G>A in one PC allele; the other variant could not be identified within the coding sequence and the boundary regions of the other allele and was suspected to be deep-intronic. The c.1877G>A variant was paternally inherited and causes the exchange of arginine 626 into glutamine. Enzymatic activity of pyruvate carboxylase measured in skin fibroblasts was 0.09 nm \cdot min $^{-1}\cdot$ mg $^{-1}$ protein (6% of control sample; control = 1.5 nm \cdot min $^{-1}\cdot$ mg $^{-1}$) and PC/CS ratio was 0.18 (4% of control sample; Figure 2).

Patient 4 (type C) harbors c.797C>A in one PC allele. This variant causes the exchange of serine 266 into tyrosine and was maternally inherited. In patient 4 too, the second variant could not be identified neither in the coding part nor in the boundary regions of PC and was suspected to be deep-intronic. Enzymatic activity measured in skin

FIGURE 2 Enzymatic activity of pyruvate carboxylase in skin fibroblasts. Enzymatic activity of pyruvate carboxylase was measured in skin fibroblasts of patients 2 and 3 (both type A) and patient 4 (type C) and was expressed as percentage value of the corresponding healthy control sample. One healthy control sample was used for each patient fibroblasts' measurement



fibroblasts was $0.00 \text{ nm}\cdot\text{min}^{-1}\cdot\text{mg}^{-1}$ protein (0% of control sample) and PC/CS ratio was 0 (0% of control sample; Figure 2).

The sibling patients 5 and 6 (type C) harbor two compound-heterozygous variants in PC, c.3242 A>G of maternal origin and c.751 + 4 A>G of paternal origin. The first variant causes the exchange of asparagine 1,081 into serine and the second variant is likely expected to impair the splicing of intron 5 and the synthesis of the correct polypeptide. Both variants were previously described neither as pathogenic nor as benign variants. Enzymatic activity of pyruvate carboxylase could not be measured due to missing compliance of patients' parents (Table 1).

3.3 | Structural modeling of human PC and variant mapping

The constructed homology models represent two conformers of the homotetramer: conformer 1 with the BCCP domain adjacent to the BC domain and conformer 2 where BCCP brings biotin to the CT domain. The two conformers themselves contain several substates. In the conformer 1, monomers A and B capture the position of BCCP domain between BC and CT domains (Figure 3) and monomers C and D have the BCCP domain closer to the BC domain (Figure S1); this state could be visited just before or right after carboxyl transfer to biotin. Conformer 2 also represents a combination of two substates. In all four monomers (A, B, C, and D) of the conformer 2, the BCCP domain has biotin delivered to the CT domain. However, the conformation of the BCCP domain differs between the monomers A and B (Figure 3) and monomers C and D (Figure S1). The overall motion of the pyruvate carboxylase performed during the carboxyl transfer step can be viewed in the supplementary section (Video S1). The movement of the enzyme covers $>6.4 \text{ nm}$ root mean squared displacement, when considering only the amino acid backbone atoms.

The overall variant mapping does not allow a unique classification of the phenotypic manifestation based on the localization of the

variant (Figure 3). The variants associated with type A PCD appear in the BC and CT domains, whereas type C variants are found in the BC, CT, and PT domains. Some variants are found near the ligand binding sites, for example, p.G150dup (type A) and p.S266A (type C) close to ATP, p.R451C (type A) close to acetyl-CoA, p.A610T (type A) close to pyruvate and biotin, p.M743I (type A) close to pyruvate. Other variants are located at the interface of the enzyme's monomeric subunits, for example, p.R62C (type A), p.R451C (type A), and p.N1081S (type C) are in the proximity of residues in an adjacent monomer.

3.4 | Predicted PC protein stability

To estimate how the single variant changes the PC stability and whether the protein stability degree is related to the disease phenotype, for each variant we have calculated the total double free energy difference ($\Delta\Delta G$), double free energy difference of conformer 1 ($\Delta\Delta G_{\text{conformer1}}$), double free energy difference of conformer 2 ($\Delta\Delta G_{\text{conformer2}}$), and the difference between the latter two ones ($\Delta\Delta\Delta G$) as a relative stability indicator between the two conformers (Table 2). The calculations were performed using two energy functions yielding a range of stability estimates which in turn provide an indication for prediction accuracy. In the two following sections, we report the calculated free energies for all previously reported as well as novel variants: p.R62C, p.V145A, p.R156Q, p.R270W, p.R451C, p.A610T, p.R626Q, p.R631Q, p.M743I, p.A847V (all type A variants) and p.S266A, p.S266Y, p.T569A, p.N1081S (all type C variants).

3.4.1 | Variants in type A patients

The free energy calculation suggests that the p.R62C variant not only does not distort the protein's fold, but may even have a stabilizing effect. However, a change between the conformers is introduced by the p.R62C variant, resulting in $\Delta\Delta\Delta G$ of -3.1 to -1.0 kcal/mol and favoring

TABLE 1 Molecular characterization PC gene and protein in type A and type C PCD patients

| Source | Patient | Amino acid variants | Involved protein domain(s) | Variant zygosity | Comments on mutant RNA's and protein's dysfunction | Pyruvate carboxylase's enzymatic activity |
|--|---------|--|----------------------------|-----------------------|--|---|
| Type A | | | | | | |
| This study | 1 | p.G150duplication | BC | Homozygous | | ND |
| This study | 2 | p.A610T | CT | Homozygous | Reduced protein's import into mitochondria and faster degradation | 2.3% of control sample |
| This study | 3 | p.R626Q + unknown intronic variant | CT | Compound heterozygous | Allele 2: intronic variant causing disturbed pre-mRNA splicing | 6% of control sample |
| Wexler et al. (1998) | | p.V145A | BC | Homozygous | Barely detectable amount of protein | 7–25% of control sample |
| Monnot et al. (2009) | | p.R156Q | BC | Homozygous | | ND |
| Xiang and Tong (2008); Wexler et al. (1998) | | p.R451C | BC | Homozygous | Disturbed activation by CoA | 7% of control sample |
| Carbone and Robinson (2003); Carbone et al. (1998) | | p.A610T | CT | Homozygous | Reduced protein's import into mitochondria and faster degradation | 1–4% of control sample |
| Carbone et al. (1998) | | p.M743I | CT | Homozygous | | 1–4% of control sample |
| Monnot et al. (2009) | | p.R270W + p.R631Q | BC and CT | Compound heterozygous | | ND |
| Wang et al. (2008) | | p.R62C + p.A847V + p.R631Q | BC and CT | Compound heterozygous | Three allelic variants in a somatic mosaic constellation; mutant mRNA transcripts containing r.1892 g>a and r.2540c>u were unstable and rapidly degraded | 6% of control sample |
| Type C | | | | | | |
| This study | 4 | p.S266Y + unknown intronic variant | BC | Compound heterozygous | Allele 2: unknown intronic variant supposed to disturb pre-mRNA splicing | 0% of control sample |
| This study | 5 + 6 | p.N1081S + intronic variant c.751+4A>G | PT | Compound heterozygous | Allele 2: intronic variant causing disturbed splicing of intron 5 | ND |
| Wang et al. (2008) | | p.S266A + p.S705X | BC and CT | Compound heterozygous | | 1.9% of control sample |
| Wang et al. (2008) | | p.T569A + p.L1137VfsX1170 | CT and BCCP | Compound heterozygous | | 1% of control sample |

Note. Domains: BC: biotin carboxylase; BCCP: biotin carboxyl carrier protein; CT: carboxyl transferase; mRNA: messenger RNA; ND: not determined; PT: PC tetramerization.

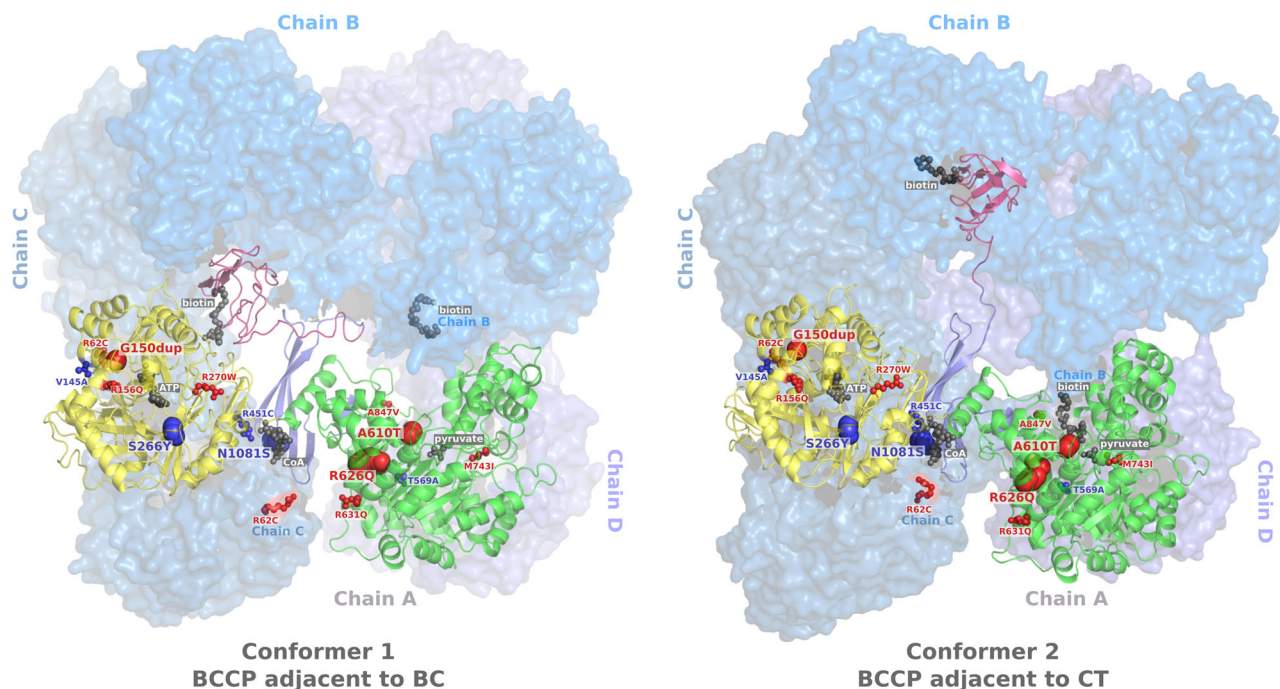


FIGURE 3 Two states of the human pyruvate carboxylase. Conformer 1 (left) has its BCCP domain in the vicinity of BC domain, while in the conformer 2 (right) BCCP domain brings biotin to the CT domain. Both structures contain four homo monomers (chains A, B, C, and D), of which monomer A is depicted in the cartoon representation, while three other monomers are in surface representation. The four domains of the monomer A are color coded: BC in yellow, CT in green, PT in violet, BCCP in pink. The ligands (ATP, biotin, CoA, and pyruvate) are depicted as gray spheres. The novel mutated residues revealed in our study are shown in big colored spheres: for type A PCD the residues are depicted in red, for type C PCD in blue. The variants previously reported in literature are depicted in small colored spheres, either red for type A PCD or blue for type C PCD. ATP: adenosine triphosphate; BC: biotin carboxylase; BCCP: biotin carboxyl carrier protein; CT: carboxyl transferase; PT: PC tetramerization

the BCCP domain interaction with the BC domain. The p.R62C variant has been referred in association to type A PCD when found in a mosaic compound-heterozygosity with p.R631Q and p.A847V variants (Table 1). p.R631Q ($\Delta\Delta G$ 2.5 kcal/mol) has a low destabilizing effect on the enzyme, while p.A847V affects the relative monomer stability ($\Delta\Delta\Delta G$ 1.2–1.5 kcal/mol) suggesting their detrimental influence on the PC function, which could be worsened by the p.R62C mutation.

The p.R631Q variant has also been implicated in another type A PCD case in compound heterozygosity with the p.R270W variant. While p.R631Q, as mentioned above, has a low destabilizing effect, p.R270W shows a potential difference among the two conformers ($\Delta\Delta\Delta G$ 0.0–6.6 kcal/mol), which may occur due to the stabilization of conformer 2 (BCCP domain interacting with the CT domain; Table 2). The variant destabilizes the interaction between BCCP and BC domains (conformer 1), which could perturb the balance between the enzyme conformations.

p.R156Q in the BC domain has a destabilizing effect on the protein, as well as altering the balance between the conformers. p.R156 is close to the ATP binding site.

The homozygous p.M743I variant has a strong destabilizing effect ($\Delta\Delta G$ 11.0–29.6 kcal/mol). The destabilization is prominent in both conformers.

The free energy calculations suggest that the p.A610T mutation is destabilizing ($\Delta\Delta G$ 2.3–6.7 kcal/mol). The major contribution to the decrease in PC stability comes from conformer 1, where biotin is

interacting with the BC domain and is not in direct contact with the variant site. This suggests that this variant may interfere with the pyruvate-enzyme interaction.

The impact of p.R626Q variant to type A PCD is difficult to explain by the calculated changes in protein stability as the predictions based on the different energy functions differ substantially. This variant appears in compound heterozygosity with an intronic mutation and it is not excluded that PCD is also caused by an incorrectly spliced protein encoded from the second allele.

p.V145A variant is strongly destabilizing as predicted by the free energy calculations ($\Delta\Delta G$ 17.0–26.1 kcal/mol). It also substantially alters the balance between the preferred conformational states in comparison to the WT enzyme: conformer 2 appears to be more stable. The p.V145 residue is in the BC domain, however it is not in direct contact with biotin.

p.R451C variant is adjacent to the acetyl-CoA binding site. The current calculations do not provide an unambiguous prediction on the mutation's effect on the enzyme's stability, nor on the balance between the conformers. As a word of caution, it has to be remarked that for the structural modeling of acetyl-CoA molecule we used the partial structure of the nonhydrolyzable analog ethyl-CoA resolved in the pyruvate carboxylase from *R. etli* (PDB 2QF7). This approximate representation of the ligand may not warrant accurate estimation of the free energy changes.

TABLE 2 Summary of free energy calculations for type A and type C variants

| Sources | Variants | Variant zygosity | $\Delta\Delta G$, kcal/mol | $\Delta\Delta G_{\text{conformer1}}$, kcal/mol | $\Delta\Delta G_{\text{conformer2}}$, kcal/mol | $\Delta\Delta\Delta G$, kcal/mol |
|--|-----------|------------------|-----------------------------|---|---|-----------------------------------|
| <i>Type A</i> | | | | | | |
| This study | p.G150dup | Homozygous | - | - | - | - |
| This study; Carbone et al. (1998) | p.A610T | Homozygous | 2.3–6.7 | 3.9–7.3 | -1.6 to -0.6 | 5.5–8.0 |
| This study | p.R626Q | Heterozygous | -12.4–3.4 | -5.3–1.7 | -7.1–1.7 | 0.0–1.8 |
| Pineda et al. (1995); Wang et al. (2008) | p.R62C | Heterozygous | -5.3–2.4 | -4.2–0.7 | -1.1–1.7 | -3.1 to -1.0 |
| Wexler et al. (1998) | p.V145A | Homozygous | 17.0–26.1 | 10.1–20.0 | 6.1–6.9 | 3.2–13.9 |
| Monnot et al. (2009) | p.R156Q | Homozygous | 2.5–50.2 | -0.8–22.0 | 3.2–28.1 | -6.1 to -4.0 |
| Monnot et al. (2009) | p.R270W | Heterozygous | -3.4–3.3 | 1.6 | -5.0–1.7 | 0.0–6.6 |
| Wexler et al. (1998) | p.R451C | Homozygous | -5.0–24.7 | -2.0–11.4 | -3.1–13.3 | -1.9–1.1 |
| Wang et al. (2008) | p.R631Q | Heterozygous | 2.5–3.4 | 1.5–1.7 | 1.0–1.7 | 0.0–0.5 |
| Carbone et al. (1998) | p.M743I | Homozygous | 11.0–29.6 | 3.7–14.9 | 7.3–14.7 | -3.6–0.3 |
| Wang et al. (2008) | p.A847V | Heterozygous | 1.4–2.2 | 1.4–1.7 | -0.1–0.5 | 1.2–1.5 |
| <i>Type C</i> | | | | | | |
| This study | p.S266Y | Heterozygous | 3.4 | 1.7 | 1.7 | 0.0 |
| This study | p.N1081S | Heterozygous | 3.3–3.4 | 1.7 | 1.6–1.7 | 0.0–0.1 |
| Wang et al. 1998; Van Coster et al. (1991) | p.S266A | Heterozygous | -7.8–2.4 | -5.0–1.3 | -2.8–1.1 | -2.2–0.2 |
| Wang et al. (2008) | p.T569A | Heterozygous | 3.3–3.4 | 1.7 | 1.7 | 0.0 |

Note. $\Delta\Delta G$ values denote changes in the PC stability calculated by thermodynamic modeling of each variant. $\Delta\Delta G_{\text{conformer1}}$ and $\Delta\Delta G_{\text{conformer2}}$ correspond to the changes in stability for the two modeled conformers. $\Delta\Delta\Delta G$ is the difference between the stability changes between the two conformers for each single variant, and represents the change in balance between the two major conformers in comparison to the WT enzyme. The free energy differences are reported as a range between the values estimated with two energy functions.

In the computational study, we could not estimate the effect of G150 duplication on PC stability, since modeling amino acid duplication would require to perform downstream sequence shifting. The residue G150 is located in the BC domain adjacent to the ATP binding site.

3.4.2 | Variants in type C patients

Variant p.S266Y destabilizes the protein ($\Delta\Delta G$ of 3.4), while it was not possible to obtain a reliable prediction of the effect of p.S266A on the enzyme's stability. Neither of the variants affects the balance between the conformers in the heterozygotic state ($\Delta\Delta\Delta G$ 0 kcal/mol and $\Delta\Delta\Delta G$ -2.2–0.2 kcal/mol, respectively). S266 residue is located in the BC domain. However, the serine side-chain is facing away from the ATP and biotin binding sites: therefore, the contribution of both mutations is mainly due to the altered interactions with the neighboring residues in the BC domain (Figures 3 and S1).

Residue p.T569 is located in the CT domain and is not in direct contact to any ligand important for the PC function. The mutation p.T569A is destabilizing ($\Delta\Delta G$ 3.3–3.4 kcal/mol) and does not affect the balance between conformer 1 and conformer 2 ($\Delta\Delta\Delta G$ 0.0 kcal/mol).

Similarly, variant p.N1081S has a small destabilizing effect on the protein ($\Delta\Delta G$ 3.3–3.4 kcal/mol). N1081 is located in the PT domain

and is in direct contact with the interface residues of another PC monomer (Figures 3 and S1), therefore it may play a role in the PC tetramerization. Interestingly, in one of the modeled states N1081 is placed closely to the R62 residue of another monomer (Figure S1) and, as discussed in the previous section, p.R62C variant has an effect on inducing type A PCD. p.N1081S variant may also have an effect on the acetyl-CoA binding: depending on the state considered, the distance between N1081 and the partial structure of ethyl-CoA is smaller than 0.5 nm.

Taken together, three out of four amino acid exchanges harbored by all reported type C patients have an overall small destabilizing effect to the enzyme (for one case, the effect on stability could not be reliably determined) and do not affect the balance between the major PC conformers. The amino acid exchanges present in type A patients manifest in a broad spectrum of the protein stability changes. The type A mutations in most cases appear to substantially disrupt the balance between the major conformational states of the enzyme, indicating a potentially detrimental effect of the genetic variant.

4 | DISCUSSION

Pyruvate carboxylase deficiency is a rare neurometabolic disease with poor correlation of genotype to phenotype, leading to difficulty

in predicting prognosis for patients. A previous study suggested that variants in the 1/3 C-terminal end of the protein could be tolerated and were unlikely to lead to disease since pathogenic missense mutations had been identified only in the 2/3 N-terminal end of the protein (Monnot et al., 2009). Additional reports have countered this observation, with compound-heterozygous mutations (p.A847V and p.L1137VfsX1170) in two patients with type A and one with type C PCD (Wang et al., 2008). We identified an N1081S variant in two patients with type C disease. Since all PCD reports from the pregenome era (Oizumi et al., 1983; Pineda et al., 1995) as well as several others from the genome era (Brun et al., 1999; García-Cazorla et al., 2006; Van Coster et al., 1998) did not describe the pathogenic mutations underlining the phenotypes, any robust hypothesis about genotype–phenotype correlation was difficult.

Some genotype–phenotype correlations seem to be valid. The mutation c.1828 G>A (p.A610T) appears to lead to type A disease, and all 13 Indo-American patients from the Canadian Cree and Ojibway tribes with this variant had infantile onset of symptoms and death within the first 5 years of life (Carbone & Robinson, 2003; Carbone et al., 1998). We reported a further Canadian patient with this mutation and type A phenotype.

p.A R631Q mutation has twice been described in patients with type A disease (Monnot et al., 2009; Wang et al., 2009). However, since this variant was in compound heterozygosity with p.R270W in one patient and with p.R62C and p.A847V in another patient, a definitive conclusion about of the p.R631Q variant remain speculative. Apart from the p.A610T variant in Canadian First Nation people, no other founder variants have been described in other populations.

As stated above, only six patients with the milder late-onset type C PCD were reported before our study and the PCD causing variants were described in only two of them (Arnold et al., 2001; Hamilton et al., 1997; Schiff et al., 2006; Van Coster et al., 1991; Wang et al., 2008). Thus, our three type C patients significantly increase our ability to examine mutations in these mild patients. Patient 4 was found to have a heterozygous mutation of serine 266 (p.S266Y), a residue previously reported to be altered in a type C patient (p.S266A; Wang et al., 2009). In our patient serine is substituted by tyrosine (p.S266Y) and in the previously reported patient serine was substituted by alanine (p.S266A), two very different amino acids. Serine 266 is the only amino acid, whose exchange has been reported more than once in association with type C disease. The difference between the two variant amino acids together with the mild phenotype in both patients suggests that the exchange of this residue only mildly alters PC function and causes a mild phenotype. This hypothesis is supported by the fact that the second variant allele in the previously reported type C patient leads to a stop-codon (p.S705X), thus leading to only one allele in this patient capable of making an abortive protein (Wang et al., 2009). Although two patients are not enough to draw any definitive conclusion, they give us an initial hint on the functional consequences of serine 266 exchange. No other mutations have been reported in more than one type C patient, and thus conclusions about their pathogenicity and

severity cannot be made. Regarding patients 5 and 6, at the current state it is difficult to speculate about the dysfunctional role of the variant c.3242 A>G (p.N1081S) just considering its position, since exchange of N1081 residue has never been reported before.

Four of six patients (patients 3, 4, 5, and 6) are compound heterozygotes, with one missense variant and one intronic variant in PC. In patients 5 and 6, the intronic variant maps at the donor splice site of intron 5. In patients 3 and 4, the intronic variant has not been localized and was estimated to have a deep-intronic position. One of these patients (patient 3) has the type A phenotype, while the rest (patients 4, 5, and 6) have the type C phenotype. Reviewing all five (former two and novel three) type C patients with revealed variants in PC, we observe that none of them harbors homozygous variants, rather all have compound-heterozygous variants. A hypothesis explaining this phenomenon might suggest that the polypeptide harboring one of the two compound-heterozygous variant amino acids is able to form a functional homotetramer, which is able in turn to exploit a sufficient enzymatic level and to produce a milder (type C) phenotype.

However, it remains unclear why some patients with compound-heterozygous variants present the fatal type A phenotype. Possibly, both compound-heterozygous variants harbored by these type A patients lead to highly impaired monomers and therefore to an overall enzyme dysfunction. To shed light on this pathophysiological hypothesis and more generally on the phenotypical consequence of homozygous missense variants in PC, it would be helpful to study patients with homozygous exchanges of residue S266 or residue T569. In fact, the computed free energy changes for these two type C associated mutations (p.S266Y and p.T569A), assuming them to be in a homozygous state, suggest a strong destabilization of the protein (>10 kcal/mol for each variant and conformer; data not shown). Furthermore, for the homozygous mutations p.S266Y and p.N1081S the balance between the monomers is predicted to be disturbed as well (data not shown). The observation of patients with homozygous variants of S266 and T569 residues—associated in heterozygous state to type C phenotype in our study—would reveal whether a severe type A phenotype rises up, either caused by the overall destabilization of the enzyme or by the disturbed balance between the major conformational states of PC or by both effects.

Another interesting scenario that could provide insight into the difference between the type A and type C phenotypes, would be an identification of the p.R631Q mutation in a heterozygous state not coupled with any additional mutations. Looking at the calculated free energy differences, p.R631Q appears to be only mildly destabilizing and to not perturb the balance between the major PC conformers. This observation would suggest its classification as a type C variant. However, coupling of this mutation to p.A847V or p.R270W results in a strong PC destabilization or in a disturbed balance between the conformers and finally in a type A phenotype (Monnot et al., 2009; Wang et al., 2008).

Independently from the associated phenotype, the mutated amino acids from patients 2, 3, 4, 5, and 6 are highly conserved throughout the evolution (Figure S2).

Several reports have concluded that there is no correlation between residual enzymatic activity in fibroblasts and patient phenotype (Stern, Nayar, Depalma, & Rifai, 1995). We were only able to measure fibroblast pyruvate carboxylase activity in patients 2 and 3 (type A phenotype) and 4 (type C phenotype), and also found activity higher in the former rather than the latter. Thus, caution is needed when discussing prognosis in newly diagnosed patients with PCD regardless of enzymatic results. It means that PC activity measurement in skin fibroblast can prove if an unknown variant impairs PC activity, but not to which extent. Of note, all of our patients had germline mutations, and thus tissue mosaicism is unlikely to be playing a role in defining phenotype as has previously been suggested (Wang et al., 2008).

In the last years, *in silico* free energy calculations have been increasingly used to estimate the effects of single amino acid mutations on protein stability and protein–ligand binding affinity (Fowler et al., 2018; Gapsys, Michielssens, Seeliger, & de Groot, 2016; Hauser et al., 2018). According to the results of our structural analysis, the close proximity of the residues G150, R451, A610, M743 (all associated to type A PCD) to the functionally relevant ligands may indicate that the respective variants could impair the interaction of the protein with the ligands (ATP, pyruvate, biotin, and acetyl-CoA) or they could potentially alter the energetics of the catalytic carboxyl transfer steps. An example supporting the hypothesis that type A variants are linked with the disturbed interactions between the enzyme and its ligands comes from patient 2 described by Monnot et al. (2009): in this case, type A phenotype is associated with the p.R631Q and p.R270W variants. p.R270W may interfere with the bicarbonate binding and biotin delivery to the BC domain.

According to our *in silico* models, variants associated with the type C PCD do not directly interact with ATP, biotin, and pyruvate. Some of these variants (p.S266A, p.S266Y, and p.T569A) are located in the core of the BC and CT domains and destabilize the enzyme. S266 is neighboring C265 which has been speculated to be important for the CO₂ fixation from the bicarbonate (Li & Cronan, 1992). This observation matches a positive response of the patient with the p.S266A variant to bicarbonate treatment (Van Coster et al., 1991). p.N1081S may have an effect on the interaction between the four PC monomers with each other or might affect the enzyme's activation by acetyl-CoA.

For most of the described variants associated to both type A and type C PCD, free energy calculations predicted a destabilizing effect of the corresponding mutant amino acid on the monomer. Interestingly, for most of the missense variants associated to type A disease the balance between the two major conformational states (conformers 1 and 2) of the enzyme is disturbed; on the contrary, for all type C missense variants the balance between the two conformers appears to be unperturbed. Taken together, we hypothesize that a missense variant, which does not cause a precocious messenger RNA decay, leads to a mutant monomer with a residual enzymatic function and to the consequent mild type C phenotype if this mutant amino acid does not disturb the balance between the two major enzyme conformers. On the

contrary, if the mutant amino acid leads to a misbalance between the two main conformers, the global enzymatic function of the mutant homotetramer is impaired to cause a severe type A phenotype.

5 | CONCLUSION

This study improves our understanding of genotype–phenotype correlation in PCD. Considering the genetic data of all reported patients with type A and C phenotypes, we could observe that a late-onset mild PCD (type C) is not associated to homozygous variants but to heterozygous ones in PC. In general, our *in silico* calculations of the PC-free energy changes show that mutations which do not destabilize the balance between the two major enzyme conformers are likely to lead to the type C phenotype, while those mutations which affect balance between the two major conformers (regardless of predicted residual enzymatic activity) lead to a type A phenotype. Identification and characterization of additional PCD patients will help to further refine these predictions.

ORCID

Emanuele G. Coci  <http://orcid.org/0000-0002-9308-2193>

Rebecca Ganetzky  <http://orcid.org/0000-0001-6238-8109>

REFERENCES

- Ahmad, A., Kahler, S. G., Kishnani, P. S., Artigas-Lopez, M., Pappu, A. S., Steiner, R., ... Van Hove, J. L. K. (1999). Treatment of pyruvate carboxylase deficiency with high doses of citrate and aspartate. *American Journal of Medical Genetics*, 87(4), 331–338.
- Alford, R. F., Leaver-Fay, A., Jeliazkov, J. R., O'Meara, M. J., DiMaio, F. P., Park, H., & Gray, J. J. (2017). The Rosetta all-atom energy function for macromolecular modeling and design. *Journal of Chemical Theory and Computation*, 13(6), 3031–3048.
- Arnold, G. L., Griebel, M. L., Porterfield, M., & Brewster, M. (2001). Pyruvate carboxylase deficiency. Report of a case and additional evidence for the "Mild" phenotype. *Clinical Pediatrics*, 40(9), 519–521.
- Atkin, B. M., Utter, M. F., & Weinberg, M. B. (1979). Pyruvate carboxylase and phosphoenolpyruvate carboxykinase activity in leukocytes and fibroblasts from a patient with pyruvate carboxylase deficiency. *Pediatric Research*, 13(1), 38–43.
- Breen, C., White, F. J., Scott, C. A., Heptinstall, L., Walter, J. H., & Morris, A. A. (2014). Unsuccessful treatment of severe pyruvate carboxylase deficiency with triheptanoin. *European Journal of Pediatrics*, 173(3), 361–366.
- Brun, N., Robitaille, Y., Grignon, A., Robinson, B. H., Mitchell, G. A., & Lambert, M. (1999). Pyruvate carboxylase deficiency: Prenatal onset of ischemia-like brain lesions in two sibs with the acute neonatal form. *American Journal of Medical Genetics*, 84(2), 94–101.
- Carbone, M. A., MacKay, N., Ling, M., Cole, D. E. C., Douglas, C., Rigat, B., & Robinson, B. H. (1998). Amerindian pyruvate carboxylase deficiency is associated with two distinct missense mutations. *The American Journal of Human Genetics*, 62(6), 1312–1319.
- Carbone, M. A., Applegarth, D. A., & Robinson, B. H. (2002). Intron retention and frameshift mutations result in severe pyruvate carboxylase deficiency in two male siblings. *Human Mutation*, 20(1), 48–56.
- Carbone, M. A., & Robinson, B. H. (2003). Expression and characterization of a human pyruvate carboxylase variant by retroviral gene transfer. *Biochemical Journal*, 370(1), 275–282.

- Fowler, P. W., Cole, K., Gordon, N. C., Kearns, A. M., Llewelyn, M. J., Peto, T. E. A., & Walker, A. S. (2018). Robust prediction of resistance to trimethoprim in *Staphylococcus aureus*. *Cell Chemical Biology*, 25(3), 339–349.
- Gapsys, V., Michielsens, S., Seeliger, D., & de Groot, B. L. (2016). Accurate and rigorous prediction of the changes in protein free energies in a large-scale mutation scan. *Angewandte Chemie International Edition*, 55(26), 7364–7368.
- García-Cazorla, A., Rabier, D., Touati, G., Chadeaux-Vekemans, B., Marsac, C., de Lonlay, P., & Saudubray, J. M. (2006). Pyruvate carboxylase deficiency: Metabolic characteristics and new neurological aspects. *Annals of Neurology*, 59(1), 121–127.
- Hamilton, J., Rae, M. D., Logan, R. W., & Robinson, P. H. (1997). A case of benign pyruvate carboxylase deficiency with normal development. *Journal of Inherited Metabolic Disease*, 20(3), 401–403.
- Hauser, K., Negron, C., Albanese, S. K., Ray, S., Steinbrecher, T., Abel, R., & Wang, L. (2018). Predicting resistance of clinical Abl mutations to targeted kinase inhibitors using alchemical free-energy calculations. *Communications Biology*, 1, 70.
- Higgins, J. J., Glasgow, A. M., Lusk, M., & Kerr, D. S. (1994). MRI, clinical, and biochemical features of partial pyruvate carboxylase deficiency. *Journal of Child Neurology*, 9(4), 436–439.
- Higgins, J. J., Ide, S. E., Oghalai, J. S., & Polymeropoulos, M. H. (1997). Lack of mutations in the biotin-binding region of the pyruvate b carboxylase (PC) gene in a family with partial PC deficiency. *Clinical Biochemistry*, 30(1), 79–81.
- Kellogg, E. H., Leaver-Fay, A., & Baker, D. (2011). Role of conformational sampling in computing mutation-induced changes in protein structure and stability. *Proteins*, 79(3), 830–838.
- Li, S. J., & Cronan, J. E., Jr. (1992). The gene encoding the biotin carboxylase subunit of *Escherichia coli* acetyl-CoA carboxylase. *Journal of Biological Chemistry*, 267(2), 855–863.
- Marin-Valencia, I., Roe, C. R., & Pascual, J. M. (2010). Pyruvate carboxylase deficiency: Mechanisms, mimics and anaplerosis. *Molecular Genetics and Metabolism*, 101(1), 9–17.
- Mochel, F., DeLonlay, P., Touati, G., Brunengraber, H., Kinman, R. P., Rabier, D., & Saudubray, J. M. (2005). Pyruvate carboxylase deficiency: Clinical and biochemical response to anaplerotic diet therapy. *Molecular Genetics and Metabolism*, 84(4), 305–312.
- Monnot, S., Serre, V., Chadeaux-Vekemans, B., Aupetit, J., Romano, S., De Lonlay, P., & Bonnefont, J. P. (2009). Structural insights on pathogenic effects of novel mutations causing pyruvate carboxylase deficiency. *Human Mutation*, 30(5), 734–740.
- Oizumi, J., Shaw, K. N. F., Giudici, T. A., Carter, M., Donnell, G. N., & Ng, W. G. (1983). Neonatal pyruvate carboxylase deficiency with renal tubular acidosis and cystinuria. *Journal of Inherited Metabolic Disease*, 6(3), 89–94.
- Ortez, C., Jou, C., Cortès-Saladelafont, E., Moreno, J., Pérez, A., Ormazábal, A., & García-Cazorla, A. (2013). Infantile parkinsonism and GABAergic hypotransmission in a patient with pyruvate carboxylase deficiency. *Gene*, 532(2), 302–306.
- Pineda, M., Campistol, J., Vilaseca, M. A., Briones, P., Ribes, A., Temudo, T., & Rolland, M. O. (1995). An atypical French form of pyruvate carboxylase deficiency. *Brain & Development*, 17(4), 276–279.
- Robinson, B. H., Toone, J. R., Petrova-Benedict, R., Dimmick, J. E., Oei, J., & Applegarth, D. A. (1985). Prenatal diagnosis of pyruvate carboxylase deficiency. *Prenatal Diagnosis*, 5(1), 67–71.
- Robinson, B. H., Oei, J., Saudubray, J. M., Marsac, C., Bartlett, K., Quan, R., & Gravel, R. (1987). The French and North American phenotypes of pyruvate carboxylase deficiency, correlation with biotin containing protein by (3)H-biotin incorporation, (35)S-streptavidin labeling, and Northern blotting with a cloned cDNA probe. *The American Journal of Human Genetics*, 40(1), 50–59.
- Sali, A., & Blundell, T. L. (1993). Comparative protein modelling by satisfaction of spatial restraints. *Journal of Molecular Biology*, 234(3), 779–815.
- Schiff, M., Levrat, V., Acquaviva, C., Vianey-Saban, C., Rolland, M. O., & Guffon, N. (2006). A case of pyruvate carboxylase deficiency with atypical clinical and neuroradiological presentation. *Molecular Genetics and Metabolism*, 87(2), 175–177.
- Stern, H. J., Nayar, R., Depalma, L., & Rifai, N. (1995). Prolonged survival in pyruvate carboxylase deficiency: Lack of correlation with enzyme activity in cultured fibroblasts. *Clinical Biochemistry*, 28(1), 85–89.
- St Maurice, M., Reinhardt, L., Surinya, K. H., Attwood, P. V., Wallace, J. C., Cleland, W. W., & Rayment, I. (2007). Domain architecture of pyruvate carboxylase, a biotin-dependent multifunctional enzyme. *Science*, 317(5841), 1076–1079.
- Van Coster, R. N., Fernhoff, P. M., & De Vivo, D. C. (1991). Pyruvate carboxylase deficiency: A benign variant with normal development. *Pediatric Research*, 30, 1–4.
- Van Coster, R. N., Janssens, S., Misson, J. P., Verloes, A., & Leroy, J. G. (1998). Prenatal diagnosis of pyruvate carboxylase deficiency by direct measurement of catalytic activity on chorionic villi samples. *Prenatal Diagnosis*, 18(10), 1041–1044.
- Wang, D., & De Vivo, D. (2009). M. P. Adam, H. H. Ardinger, R. A. Pagon, S. E. Wallace, L. J. H. Bean, K. Stephens, & A. Amemiya (Eds.), *Pyruvate carboxylase deficiency*. Seattle, Washington, DC.: University of Washington.
- Wang, D., Yang, H., De Braganca, K. C., Lu, J., Shih, L. Y., Briones, P., & De Vivo, D. C. (2008). The molecular basis of pyruvate carboxylase deficiency: Mosaicism correlates with prolonged survival. *Molecular Genetics and Metabolism*, 95(1-2), 31–38.
- Wallace, J. C., Jitrapakdee, S., & Chapman-Smith, A. (1998). Pyruvate carboxylase. *International Journal of Biochemistry & Cell Biology*, 30(1), 1–5.
- Wexler, I. D., Kerr, D. S., Du, Y., Kaung, M. M., Stephenson, W., Lusk, M. M., & Higgins, J. J. (1998). Molecular characterization of pyruvate carboxylase deficiency in two consanguineous families. *Pediatric Research*, 43(5), 579–584.
- Xiang, S., & Tong, L. (2008). Crystal structures of human and *Staphylococcus aureus* pyruvate carboxylase and molecular insights into the carboxyltransfer reaction. *Nature Structural & Molecular Biology*, 15(3), 295–302.

SUPPORTING INFORMATION

Additional supporting information may be found online in the Supporting Information section at the end of the article.

How to cite this article: Coci EG, Gapsys V, Shur N, et al. Pyruvate carboxylase deficiency type A and type C: Characterization of five novel pathogenic variants in PC and analysis of the genotype–phenotype correlation. *Human Mutation*. 2019;40:816–827. <https://doi.org/10.1002/humu.23742>